Fusion enhancement in the ^{32,38}S+^{181}Ta reaction

K. E. Zyromski,[1,*] W. Loveland,[1] G. A. Souliotis,[1,†] D. J. Morrissey,[2] C. F. Powell,[2] O. Batenkov,[3] K. Aleklett,[4]
R. Yanez,[4] and I. Forsberg[1]

[1]*Department of Chemistry, Oregon State University, Corvallis, Oregon 97331*
[2]*National Superconducting Cyclotron Laboratory, Michigan State University, East Lansing, Michigan 48824*
[3]*Khlopin Radium Institute, St. Petersburg, Russia*
[4]*Uppsala University, Uppsala, Sweden*

We measured the capture-fission excitation functions for the ^{32}S+^{181}Ta reaction and the ^{38}S+^{181}Ta reaction. (The radioactive ^{38}S beam was produced by projectile fragmentation.) In the ^{32}S-induced reaction, an incomplete fusion component was observed at high energies, with an average linear momentum transfer corresponding to the escape of an α particle. The deduced interaction barrier heights were 130.7 ± 0.3 and 124.8 ± 0.3 MeV for the ^{32}S- and ^{38}S-induced reactions, respectively. No differences between the two reactions were observed beyond a simple shift in the interaction barrier height.

I. INTRODUCTION

One of the interesting aspects of the study of nuclear reactions induced by radioactive beams is the possibility of using *n*-rich radioactive projectiles to synthesize new, neutron-rich heavy nuclei [1]. It has been shown [2] that new areas in the atomic physics and chemistry of the transactinide elements could be developed using intense *n*-rich radioactive beams.

Various authors [3–6] have suggested that there will be significant enhancements to the fusion cross sections for *n*-rich projectiles due to the lowering of the fusion barrier, the excitation of the soft dipole mode, and the lowering of the reaction Q values for the more *n*-rich projectiles. The survival probability of the evaporation residues (EVRs) is also expected to increase due to their reduced fissionability and lowered excitation energy.

They have further speculated that the use of these projectiles might lead to the successful synthesis of new or superheavy nuclei. Takigawa *et al.* [3] predict an enhancement of 10^5 in the fusion cross section for the ^{46}K+^{238}U reaction compared to the ^{41}K+^{238}U reaction and an increase of a factor of 2 in the survival probabilities for the EVRs. Experience from the synthesis of new heavy nuclei by nonradioactive *n*-rich projectiles shows that an increase of one unit in isospin of the projectile increases the heavy element production cross sections by a factor of 5 [7].

Several new radioactive beam facility proposals have focused, in part, on these possible attractive features of using *n*-rich radioactive beams. The goal of this project was to make a measurement of the fusion enhancement factors for radioactive *n*-rich projectiles of interest in the synthesis of new heavy nuclei.

There have been several studies [8–19] of the effect of varying the isospin of the projectile and the target nuclei upon the fusion cross section. In some of these studies [14],

the effect of the changing isospin was a simple shift in the fusion barrier with similar reduced excitation functions for the systems under study. For reactions at sub-barrier energies, however, more complicated nuclear structure effects appear to play a role. These have been described [9,10,13,15–19] in terms of inelastic excitations of the projectile and target nuclei and the influence of transfer reaction channels. Alternate explanations [20,21] use a macroscopic description of neck formation or neutron flow to explain the observed effects of *N/Z* upon the fusion process.

One of the first reported studies of the effect of using radioactive *n*-rich medium-mass projectiles to produce heavy nuclei was the preliminary report of Yoshida *et al.* (communicated by Signorini [22]). This study of the ^{27,29,31}Al+^{197}Au reaction showed the expected shift in the excitation functions due to a lowered fusion barrier for the *n*-rich projectiles. The observations with the radioactive beams were not well described by coupled channel calculations. In a short, preliminary version of this paper, Zyromski *et al.* [23], reported fusion excitation functions for the ^{32,38}S+^{181}Ta reaction. This study concluded that the use of the *n*-rich projectile led to simple lowering of the fusion barrier with the reduced excitation functions for the two reactions being identical within experimental uncertainties.

This paper represents an expansion and extension of the previous report of the ^{32,38}S+^{181}Ta reaction [23]. In this work, we report in greater detail the experimental design used to measure fusion excitation functions with low intensity, high energy radioactive beams from a projectile fragmentation facility. We also correct some errors in the previous analysis, demonstrate the existence of a previously unrecognized incomplete fusion component of the cross sections, and extract quantitatively different values of the interaction barriers using a less model-dependent analysis. We explain, in detail, our attempts at corrections for quasifission. While the quantitative conclusions of this work differ from Ref. [23], the qualitative conclusions remain the same.

In Sec. II of this paper, we describe the experimental methods used. In Sec. III, we discuss the results and the correction for quasifission, In Sec. IV, we present our con-

---

*Present address: Isotope Products Laboratories, Burbank, CA.

†Present address: Texas A&M University, College Station, TX.

clusions and comment on their potential significance in the synthesis of new heavy nuclei.

II. EXPERIMENTAL METHODS

A. Design of experiment

A readily available *n*-rich projectile that can act as a prototype for the projectiles likely to be involved in future heavy element synthesis is ^{38}S. ^{38}S ($t_{1/2} \simeq 170$ m) can be produced by fragmentation of ^{40}Ar using the A1200 radioactive beam facility at the National Superconducting Cyclotron Laboratory (NSCL) at Michigan State University. By measurement and comparison of fusion cross sections and excitation functions for the fusion of stable ^{32}S and radioactive ^{38}S with ^{181}Ta, we can evaluate quantitatively the expected fusion enhancement factors. ^{38}S ($N/Z = 1.38$) is as neutron rich as any radioactive projectile nucleus currently available in reasonable intensities from radioactive beam facilities [24]. Comparison of its fusion properties with those of ^{32}S ($N/Z = 1$) should be a meaningful comparison. Neither ^{32,38}S or ^{181}Ta are ''magic'' nuclei, and thus any special effects due to shell stabilization will not be present. PACE calculations [25] indicated that greater than 99% of the products formed in this reaction decay by fission, so the fusion–fission excitation function should be equivalent to the fusion excitation function.

B. Stable beam experiment

The ^{32}S + ^{181}Ta experiment was performed at the ATLAS accelerator at Argonne National Laboratory. Well-focused, well-collimated beams of ^{32}S with intensities of 4 to 8 enA were sent to the 36 in. scattering chamber where the experimental apparatus was arranged. Measurements were made at 16 beam energies ranging from 157 to 300 MeV; the measurements were made in two separate passes through the range of energies in order to avoid possible systematic error. All energy changes were made in the accelerator, with no additional energy degradation at the chamber. A typical beam energy resolution was 0.01 to 0.1 MeV, and so direct measurement of time of flight (TOF) of the beam particles was unnecessary. (Beam energy and resolution at ATLAS are determined continuously by multiple TOF measurements of the arrival of beam bunches at various points along the beamline.) A satellite beam, nominally identified by TOF and energy to be ^{16}O, was observed as scattered beam in the most forward detectors, but it was a very small component (on the order of 10^{-9} of the total beam) and was easily separable in the data analysis.

In the scattering chamber, 16 300 mm^2 silicon surface-barrier detectors of thickness 60 to 100 μm were arranged in a plane at angles from 15° to 160° in the lab frame, at a distance of 170 mm from the target. Each detector subtended 10.4 msr, and so the total solid angle covered by the detector array was 1.3% of 4π. The target ladder in the center of the chamber contained an 0.46 mg/cm^2 self-supporting ^{181}Ta target. The beam current was monitored by counting the elastically scattered beam particles at angles inside the grazing angle and normalizing this to the Rutherford scattering cross section. The beam current for a typical run was $1.5-3 \times 10^9$ ^{32}S per second, giving event rates from 250–300 fission fragments per minute in the most forward detectors to 50–100 per minute in the most backward detectors. Measurements of one half hour to one hour per energy were made in order to obtain adequate numbers of events.

C. Radioactive beam experiments

The capture-fission excitation function for the radioactive beam ^{38}S + ^{181}Ta reaction was measured in two separate experiments at the National Superconducting Cyclotron Laboratory (NSCL) at Michigan State University. Beams from the K1200 cyclotron were fragmented, and the secondary radioactive beam was separated and degraded in energy in the A1200 fragment separator. After separation, the beam was sent to the 92 in. scattering chamber where the experimental setup was located. In the chamber, the beam energy was further degraded, beam characteristics were observed, and measurement of the fusion reaction took place.

Radioactive beams are produced at the NSCL by the projectile fragmentation method, in which a high-energy primary beam impinges on a light target and the resulting fragments continue forward at velocities near that of the primary beam. For these experiments, the primary beam was ^{40}Ar at 40 MeV/nucleon and the production target was 141 mg/cm^2 ^{9}Be. The desired secondary beam (in this case, ^{38}S) is then selected from the fragmentation products using the A1200 magnetic separator, and sent to the experimental area.

After separation in the A1200, the secondary ^{38}S beam, with a final energy ~ 8 MeV/nucleon (as measured by time of flight in the A1200), was sent to the 92 in. scattering chamber. The experimental setup inside the 92 in. chamber consisted of a degrader wheel, two pairs of detectors for beam timing and imaging, a set of fission detectors, and a silicon detector at the end of the beamline to monitor beam intensity and characteristics. A schematic diagram of the apparatus is shown in Fig. 1. At the entrance to the chamber a wheel with 12 holes of 3 cm diameter was mounted. Aluminum foils ranging in thickness from 1.6 to 14 mg/cm^2 were mounted over 11 of these holes to degrade the ^{38}S beam from 8 MeV/nucleon to the desired reaction energies. The wheel was attached to a stepper motor so that rotation of the foils into the beamline could be controlled from outside the chamber. After the beam passed through the degrader, an image of the beam spot was obtained using an *x*-*y* position-sensitive parallel-plate avalanche counter (PPAC) detector [26] with a 5 cm × 5 cm active area, which also served as the first element of the beam timing system. The beam spot for a typical run from the second experiment was 1.5 to 2 cm in diameter after degradation in the chamber.

The beam timing system consisted of two pairs of detectors mounted on a support arm extending roughly one meter from the beam entrance to the table supporting the fission detectors. For the second experiment, the support arm was mounted on a movable rail, so that the entire beam timing system could be rotated out of the path of the beam during high-intensity stable-beam calibration runs. The outer pair of timing detectors were PPACs: the beam-imaging PPAC
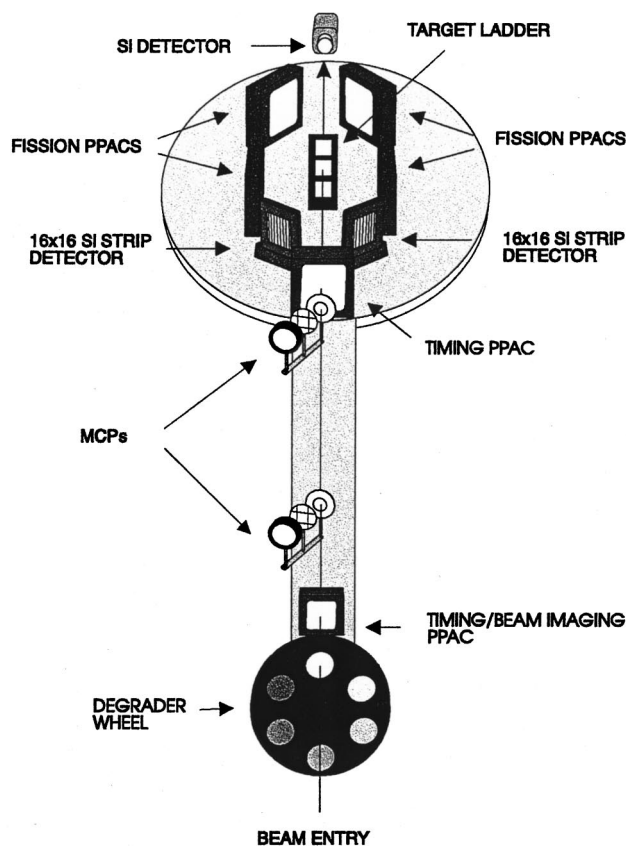
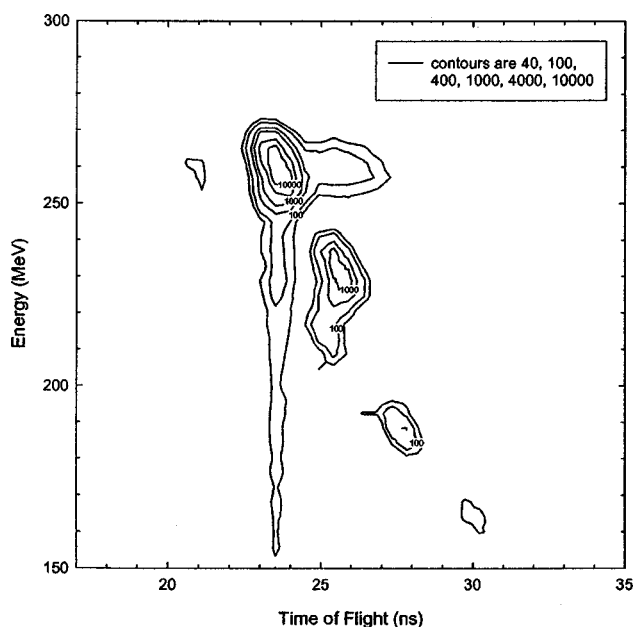FIG. 1. Schematic diagram of experimental apparatus used in radioactive beam measurements.

FIG. 2. A plot of the time of flight vs energy for the undegraded radioactive beam showing the primary ^{38}S beam and satellite imputities.

mentioned previously and a second 10 cm$\times$10 cm PPAC located 114 cm downstream, from which no imaging signals were taken. Between the PPACs were a pair of microchannel plate detectors (MCPs) [27] separated by a flight path of 93 cm (97 cm in the second experiment). Thin aluminum or aluminum oxide foils were placed in the beamline at an angle of 45° as electron emitter foils for the MCPs, and wire grids were used to focus the electrons onto the MCPs. In the first experiment, the emitter foil thicknesses were 3.09 mg/cm^2 Al (upstream) and 60 μg/cm^2 Al$_2$O$_3$ (downstream); in the second experiment, both emitter foils were 1.62 mg/cm^2 Al. The MCPs themselves were set at backward angles out of the beamline. 1.75 cm diameter collimators were placed in front of the MCPs during the second experiment to reduce scattered beam background. The time resolution of the PPAC timing system was 1.5 ns FWHM for the one-meter flight path, and the MCP timing system had a timing resolution of 530 ps FWHM, as measured using a stable ^{40}Ar beam of 300.9 MeV. (The beam energy spectrum in the Si detector at the end of the beamline had a FWHM of 2.5 MeV, which corresponds to a spread in TOF of 100 ps.)

Efficiency of the timing system was calibrated by measuring the percentage of ^{38}S beam particles implanted in the silicon detector at the end of the beamline, which had triggered a coincidence signal in the ^{38}S TOF peak for each pair of timing detectors. The efficiency of the MCPs was 95%–99%, and PPAC efficiency was measured to be >99%. Both of the timing systems together recorded 99.9% of the ^{38}S

beam particles. The ^{38}S rates in the silicon detector were about 500 particles/s for these runs, and the total beam rates were less than 700/s, time-averaged over the runs. Because of the low beam intensity, the beam timing system could be used to give event-by-event TOF information for the radioactive beam. The MCPs were used as the primary source of timing data due to their better resolution, with the PPACs as a backup system.

After passing through the timing system, the beam struck a 2 cm$\times$2 cm ^{181}Ta target in the center of the chamber. The targets were self-supporting, with a mean thickness of 0.924 mg/cm^2 for the first experiment and 0.857 mg/cm^2 for the second.

Two 500 μm 16$\times$16 silicon strip detectors were placed at backward angles from the target with the p+ (vertical strips) side facing the target. The detectors were at $\pm$155°(lab), at a distance of 14.6 cm. Each detector had an active area of 47 mm$\times$47 mm and covered 0.101 sr solid angle; the strips were chained together into a 4 vertical$\times$1 horizontal configuration. For the second experiment, the strip detectors were removed and replaced by an array of silicon surface barrier detectors. Eight 300 mm^2 Si detectors of 100 μm thickness were used, mounted four on each side of the beam in a square configuration which subtended 75% of the original strip detector's solid angle coverage. The signals from the strips and Si detectors were used to detect fission fragments at backward angles, but also to look for alpha particles from any heavy residues that may have survived. No residue alphas were observed for any of the data runs, which puts an upper limit on the heavy residue cross section of 3% of all events.

Four 10 cm$\times$10 cm x-y position-sensitive PPACs were placed around the target in order to detect fission fragments. Two detectors were centered at 25° (lab frame) at a distance

of 20 cm from the target, and two were at 90° and a distance of 6.5 cm. The position resolution of the PPACs was ≤5 mm as measured using a plastic mask and a ^{252}Cf calibration source. The PPACs were filled with isobutane gas at 5 to 8 torr and had applied voltages from 500 to 750 V. The four ''fission PPACs'' covered a total solid angle of 20% of 4π in the lab frame; this large area coverage was crucial to compensate for the low beam intensities. The efficiencies of these four detectors for fission fragments ranged from 85% to 88% as measured with a ^{252}Cf source. Although the PPACs subtended large solid angles and gave position information, they are transmission detectors, and so the total energy of the incident particles was not recorded. Since the detectors were also sensitive to other reaction products such as scattered beam, transfer products, and target recoils, separation of fusion–fission from other events had to be accomplished by observing angular correlations between pairs of coincident particles.

Another Si surface barrier detector with area 100 mm^2 and thickness 500 μm was placed downstream from the target. This detector was mounted on an arm attached to a movable rail, and was placed in the beam path to observe the intensity and characteristics of the radioactive beam. The rail on which this detector was mounted, which also acted as the base for the timing apparatus as mentioned previously, enabled the entire set of detectors for timing and beam imaging to be rotated out of the beamline for high-intensity stable-beam calibration runs. At the end of the beamline, a Faraday cup was attached to the exit line from the chamber. This was connected to a current integrator in the data acquisition area, and was used to measure beam current for the high-intensity calibration beams.

The total efficiency of the detector system was determined by measurement of the known fission cross section for the reaction of ^{16}O + ^{197}Au [28] at two energies. Two calibrations were made at each energy, a high beam intensity run
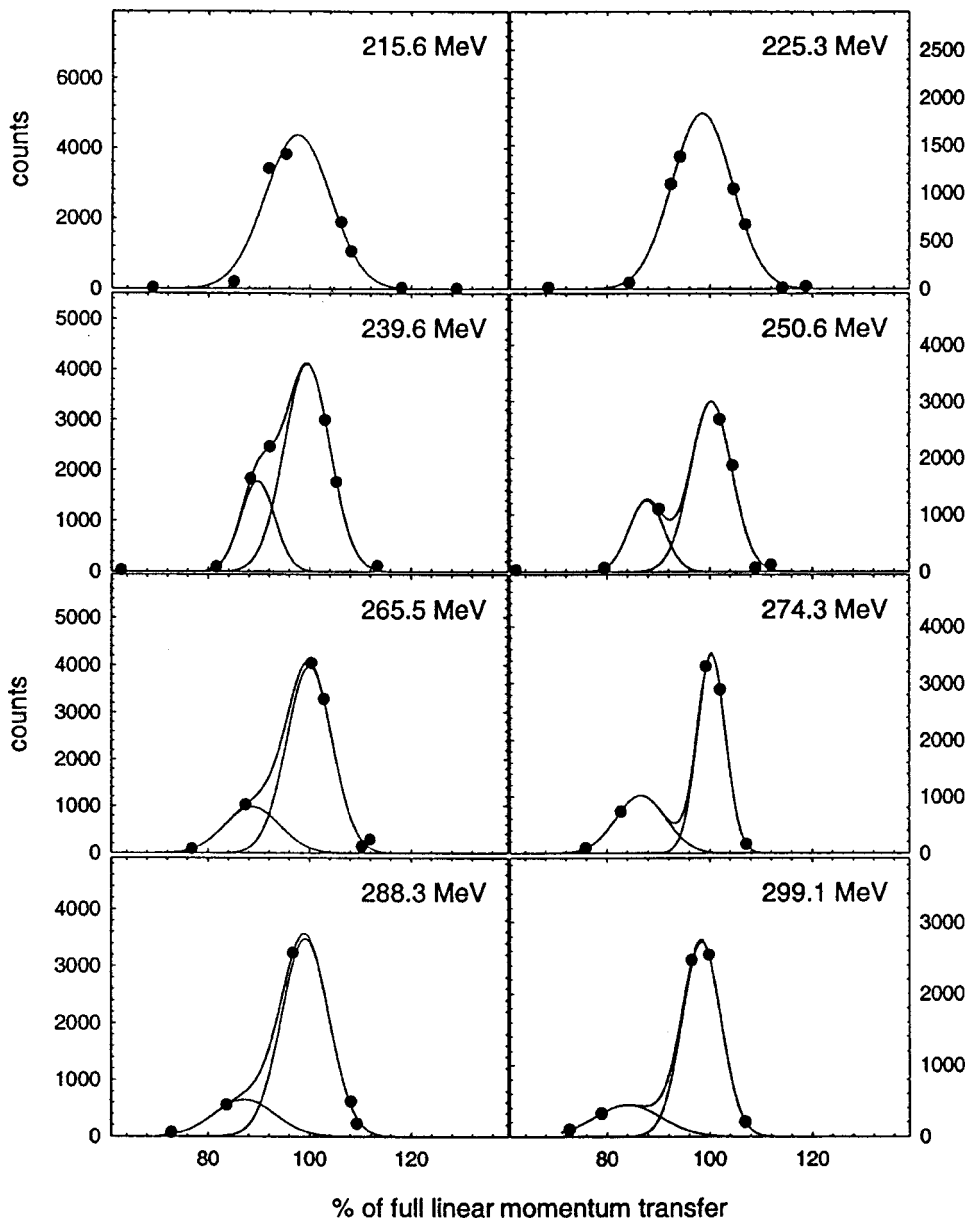

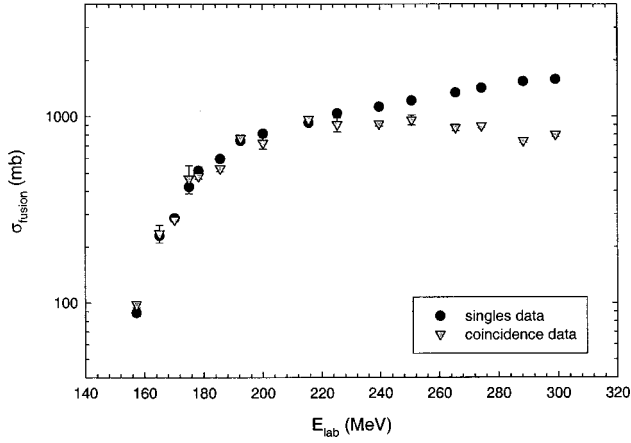FIG. 3. Fission fragment folding angle distributions for the ^{32}S + ^{181}Ta reaction.

FIG. 4. Capture fission excitation function for the ^{32}S$+$^{181}Ta reaction as deduced from singles and coincidence measurments (which excluded incomplete fusion events.)

with the beam timing system out of the beam in order to calibrate the fission PPACs and a run with beam intensities attenuated to a few thousand particles per second, to determine the efficiency of the entire fission and beam timing system. In both calibrations, valid events were determined by requiring the observation of coincident fission fragments with full momentum transfer; for the low intensity runs in the radioactive-beam configuration, an additional requirement of a trigger in the beam TOF gate of the timing system was added. The efficiency of the entire detector system was measured to be 78% ±4%.

A plot of energy versus TOF for the radioactive beam as it entered the scattering chamber is shown in Fig. 2 It can be seen that, although the ^{38}S is the major component of the beam, there are several satellite impurities as well. (The primary satellites were nominally identified as ^{39,40}S and ^{37}Si,

TABLE I. Measured cross sections for $X+$^{181}Ta.

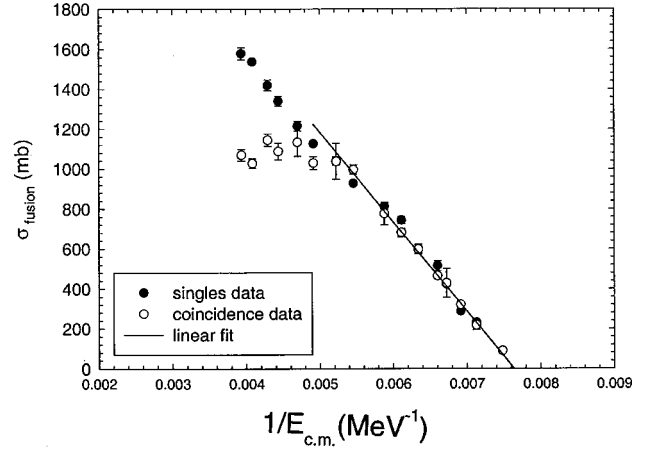| ^{32}S		^{38}S	
E_{lab}(MeV)	σ_f(mb)	E_{lab}(MeV)	σ_f(mb)
157.3	88$\pm$4	161.2	280$\pm$140
165.1	220$\pm$20	182.7	810$\pm$410
170.2	320$\pm$10	190.5	950$\pm$100
175.1	430$\pm$70	204.3	1380$\pm$260
178.3	460$\pm$20	237.7	1670$\pm$160
185.6	600$\pm$20	254.0	1620$\pm$180
192.5	680$\pm$20		
200.1	780$\pm$60		
215.6	1000$\pm$20		
225.3	1040$\pm$90		
239.6	1030$\pm$30		
250.6	1130$\pm$70		
265.5	1090$\pm$40		
274.3	1150$\pm$30		
288.3	1030$\pm$20		
299.1	1070$\pm$30		

FIG. 5. 1/E plot for the ^{32}S$+$^{181}Ta capture fission data.

based on TOF and dE/dx measurements.) Maximum beam intensities on target ranged from 2000 to 10 000 particles/s, with the ^{38}S as 85%–90% of the total flux. In order to be sure that the observed fission fragments were induced by the ^{38}S beam, event-by-event TOF information was used. A triple coincidence of timing-fission-fission was required to define a valid event. Time-of-flight gates were then used in the data analysis to associate fission-fission coincidences with the ^{38}S or with the satellite beams. True fusion-fission events (as defined by correct folding angle and coincidence with a ^{38}S particle through the timing detectors) occurred at rates ranging from about two per hour at the highest energies to roughly one event every 2.5 hours at the lowest energies. Running times were from 7–16 hours of data per energy.

III. RESULTS AND DISCUSSION

A. Stable beam experiment

In the first preliminary communication of the results of this experiment, we reported capture-fission cross sections for the ^{32}S$+$^{181}Ta reaction based on integrating the singles fission angular distributions for these reactions. Because of
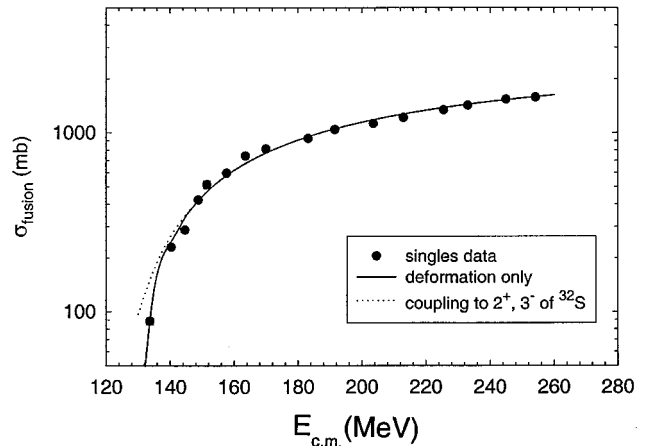

FIG. 6. Coupled channels fit to the ^{32}S$+$^{181}Ta capture fission excitation function.
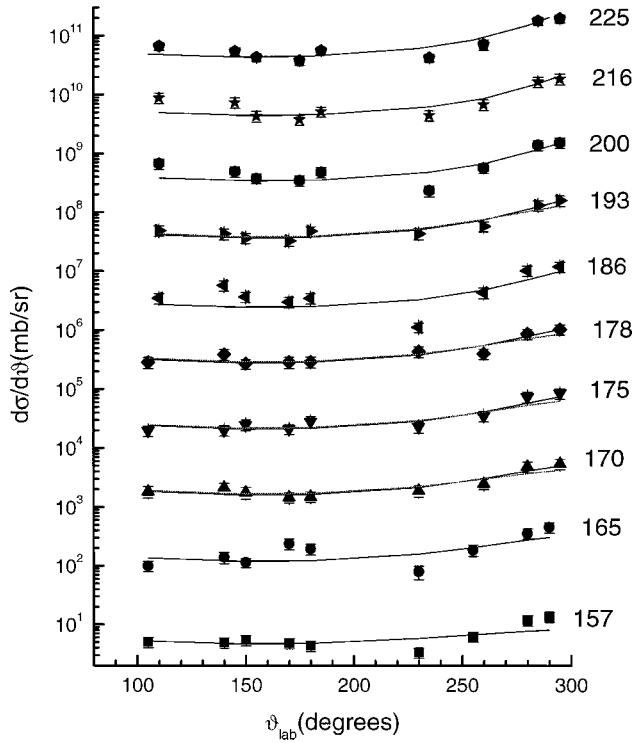
FIG. 7. Attempted fit to the fission fragment angular distributions to determine the fraction of the cross section due to quasifission for $157 \leq E_{proj} \leq 225$ MeV. For energies where only one curve is shown, the fit is not statistically significant at the 95% confidence level. For the other energies, two statistically significant fits are shown, corresponding to 0% quasifission (dashed cirve) and 100% quasifission (solid line).

the possibility of having fission induced by incomplete fusion or other processes included in this cross section, we reanalyzed these data demanding that all fission events correspond to full momentum transfer events. This was done by requiring that both fragments from a fission event be detected and that the measured folding angle be within $\pm 10\%$ of that corresponding to full linear momentum transfer. For the ten lowest projectile energies (157.3–225 MeV), a single peak was observed in the folding angle distributions, corresponding to full linear momentum transfer. At projectile energies of 239 MeV and above, a ''shoulder'' in the folding angle distributions corresponding to $\sim 87\%$ linear momentum transfer was observed (Fig. 3). At these energies, the average linear momentum transfer for the ''shoulder events'' is consistent with the fusion of an $A = 28$ fragment with the target nucleus, suggesting the possible escape of an α-particle prior to fusion. After subtracting this incomplete momentum transfer component from the measured cross sections, the resulting capture fission excitation function is shown in Fig. 4 and Table I. (In Fig. 4, we also show the previously published singles excitation function which has been corrected for errors in the analysis of the Rutherford scattering data.) The incomplete momentum transfer component corresponds to 15%–30% of the total fission cross section at the highest energies.

In these reactions, the compound nucleus is ^{213}Ac, formed at excitation energies of 47–174 MeV. According to PACE
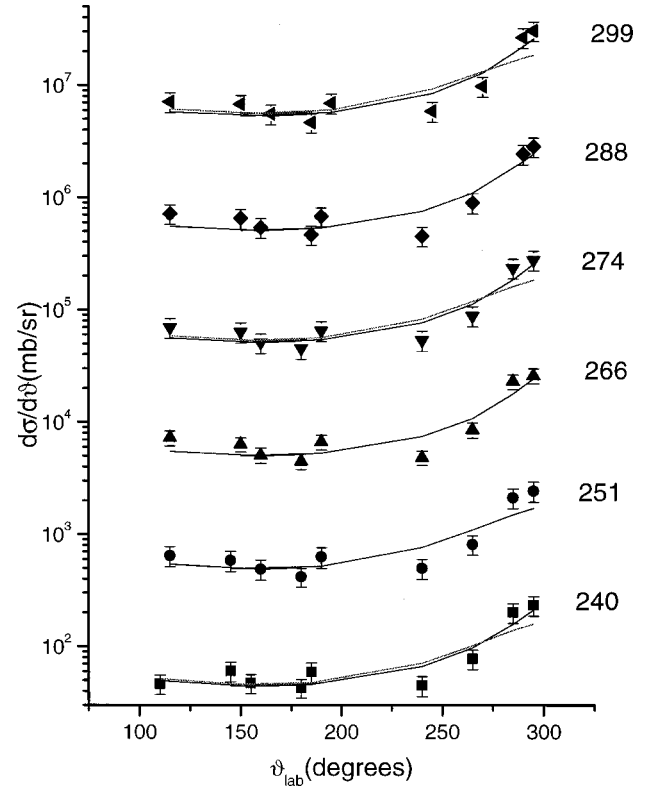

FIG. 8. Same as Fig. 7, except $240 \leq E_{proj} \leq 299$ MeV.

[25] simulations with a value of $a_f/a_n = 1.00$ [29] and temperature dependent values of a [30], the fraction of the reactions that leads to fission is 0.99 and it does not change appreciably with projectile energy. Furthermore, in our related study of the ^{38}S + ^{181}Ta reaction, a measured upper limit of $<2\%-3\%$ for the fraction of reactions leading to residue formation was found. In the study of a similar reaction, ^{32}S + ^{184}W, it was found that the residue cross section was 200 μb, a negligible quantity for this study [31]. Therefore, we have taken the capture-fission excitation function to be the capture excitation function for this reaction.

If we represent the interaction cross section by the simple semiclassical formula

$$\sigma = \pi R^2 (1 - V_b/E), \qquad (1)$$

we can plot the observed cross section data versus $1/E$ to determine V_b, the height of the interaction barrier, and R_b, the value of the interaction radius. Such a plot is shown in Fig. 5. The reduced χ^2 is 0.22. The values of V_b and R_b are 130.9 ± 0.5 MeV and 10.4 ± 0.3 fm. (In making this analysis, we have used data with $200 \leq \sigma \leq 800$ mb to exclude nonlinearities due to tunneling effects and coupling to other reaction modes at low energies and angular momentum limitations on the fusion process at high energies.) Similar values for V_b and R_b, 129.5 ± 1.7 MeV, and 10.2 ± 0.4 fm were obtained by making a fit to the data using a simplified coupled channels calculation with CCDEF [32] (Fig. 6). In this calculation, only the effect of the static deformation of ^{181}Ta ($\beta_2 = 0.269$, $\beta_4 = -0.090$) [33] was included. Coupling to the first 2^+ and 3^- excited states of ^{32}S (β_2

=0.336 [34], β_3=0.48 [35]) was not conclusive as there was not sufficient data below σ=100 mb where these effects could become more important. The weighted average of these two fits to the data for V_b and R_b are 130.7 ±0.3 MeV and 10.3±0.1 fm, respectively.

It has been shown [36,37] that for reactions like the ^{32,38}S$+^{181}$Ta reaction or the related ^{32}S$+^{182}$W reaction that a significant fraction of the fission events result from ''quasifission'' as well as ''true complete fusion.'' Quasifission is the process where the interacting nuclei merge to form a mononucleus but the system does not evolve inside the fission saddle point. Comparison of the fission excitation function for the combined processes with one-dimensional potentials, such as those used in coupled channels calculations, is appropriate. However, for the purpose of estimating heavy element production by complete fusion, one should try to separate the contributions of quasifission and true complete fusion in the data. Using the methods outlined in Refs. [36,37] which depend on analyzing the shape of the fission fragment angular distributions, we have attempted to estimate the relative contributions of quasifission and complete fusion to the observed cross sections. The authors of Refs. [36,37] studied the angular distributions for a large number of reactions including several that were similar to the ones studied in this work. They concluded that one could decompose the observed fission angular distributions into two components, one due to complete fusion and the other due to quasifission. The complete fusion component has an angular distribution characterized by values of the effective moment of inertia, $\mathfrak{I}_{\text{eff}}$, given by

$$\frac{\mathfrak{I}_0}{\mathfrak{I}_{\text{eff}}} = \max(a+bl^2, 0.3) \quad l \leq l_{\text{cn}} \qquad (2)$$

while the quasifission component has

$$\frac{\mathfrak{I}_0}{\mathfrak{I}_{\text{eff}}} = 1.5 \ l > l_{\text{cn}}. \qquad (3)$$

In these equations, $\mathfrak{I}_0$ is the moment of inertia of a spherical nucleus with the same A value, complete fusion is assumed to occur for partial waves $0 \leq l \leq l_{\text{cn}}$ and quasifission is assumed to occur for partial waves $l > l_{\text{cn}}$. The constants a and b were shown to depend only on the fissility of the fissioning nucleus, x' such that

$$x' = x_{\text{RLDM}} + 0.3, \qquad (4)$$

where the rotating liquid drop fissility, x_{RLDM} is given as

$$x_{\text{RLDM}} = \frac{Z^2/A}{50.883[1-1.7826[(N-Z)/A]^2]}. \qquad (5)$$

Values of a=1.07 and b=−0.0001075 were used in the calculations [36].

We fitted the observed fission fragment angular distributions for the projectile energies of 157–299 MeV, allowing the maximum angular momentum associated with complete fusion, J_{cn} to be a free parameter determined in the calculation. (J_{max} was determined by the total fission cross section.) We used the familar expressions for the fission fragment angular distributions [38]:

$$W(\theta) = \sum_{J=0}^{J_{\text{cn}}} \frac{(2J+1)^2 \ \exp[-(J+\frac{1}{2})^2 \ \sin^2\theta/4K_0^2] J_0[i(J+\frac{1}{2})^2 \ \sin^2\theta/4K_0^2]}{\text{erf}[(J+\frac{1}{2})/(2K_0^2)^{1/2}]}$$

$$+ \sum_{J=J_{\text{cn}}}^{J_{\text{max}}} \frac{(2J+1)^2 \ \exp[-(J+\frac{1}{2})^2 \ \sin^2\theta/4K_0^2] J_0[i(J+\frac{1}{2})^2 \ \sin^2\theta/4K_0^2]}{\text{erf}[(J+\frac{1}{2})/(2K_0^2)^{1/2}]}$$

assuming M=0, where J_0 is the zero order Bessel function with imaginary argument and the error function $\text{erf}[(J+1/2)/(2K_0^2)^{1/2}]$ is defined as

$$\text{erf}(x) = (2/\pi^{1/2}) \int_0^x \exp(-t^2) dt. \qquad (6)$$

The parameter K_0^2 is defined as

$$K_0^2 = T\mathfrak{I}_{\text{eff}}/\hbar^2, \qquad (7)$$

where the nuclear temperature at the saddle point T is given as

$$T = \left[\frac{E^*-B_f-E_{\text{rot}}}{A/8.5}\right]^{1/2}. \qquad (8)$$

The results of this analysis were not conclusive. While we found a minimum in χ^2 in the fitting process at each projectile energy, we found the fits to the data (shown in Figs. 7 and 8) were not definitive. At eight energies (157.3, 165.1, 185.6, 200.1, 215.6, 225.3, 265.5, and 288.3 MeV), the reduced χ^2 values were not significant at the 95% confidence level. At eight other energies (170.2, 175.1, 178.3, 192.5, 239.6, 250.6, 274.3, and 299.1 MeV), satisfactory fits (at the 95% confidence level) were obtained with a wide ranging set of values of J_{cn}, corresponding to quasifission contributions ranging from 0% to 100%. While the shapes of the fission angular distributions hint at excess numbers of events near 0° and 180° (the quasifission signature), the data do not allow a statistically significant extraction of the information. We shall, therefore, compare the measured values of the parameters of the one-dimensional interaction barriers with models for the isospin dependence of these quantities.
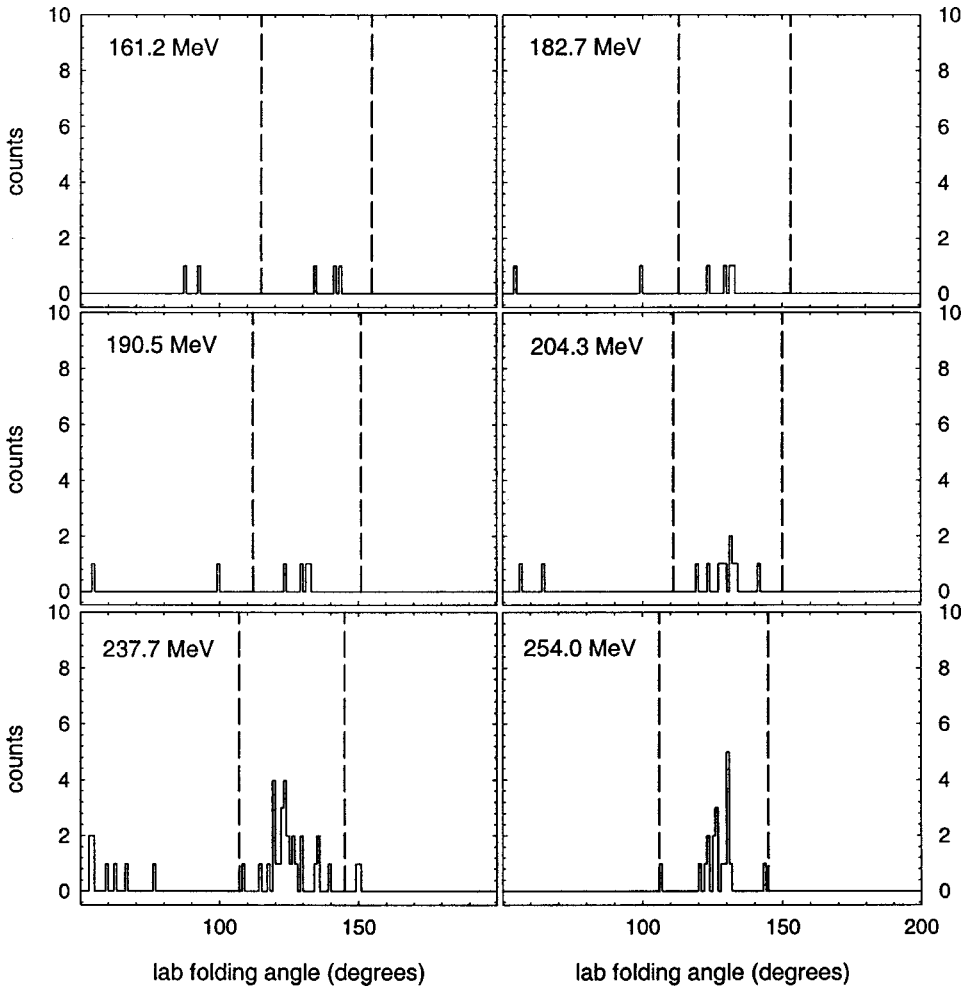
FIG. 9. Fission fragment folding angle distributions for the ^{38}S $+^{181}$Ta reaction.

B. Radioactive beam measurements

Because of the need to discriminate between scattered beam particles and fission fragments in the PPACs, only data corresponding to full linear momentum transfer events were used to determine the capture-fission cross section for the radioactive-beam reaction. The ^{38}S-gated folding angle distributions are shown in Fig. 9 along with the cuts (dashed lines) used to define full momentum transfer events. The events at small values of the folding angles correspond mostly to hits in two detectors on the same side of the beam.

The measured capture-fission cross sections for the ^{38}S $+ ^{181}$Ta reaction are shown in Fig. 10 and Table I. The silicon detectors at backward angles were used to search for any α particles emitted by evaporation residues that may have survived. No counts were observed, giving an upper limit of 3% of the capture-fission cross section at the lowest energy (182.7 MeV) and $\leq 2\%$ at $E_{\text{proj}} = 204.3$ MeV.

Assuming a negligible cross section for residue formation in this reaction, we used the same $1/E$ plots (Fig. 11) and coupled channels fit (Fig. 10) to determine values of the interaction barrier V_b and radius R_b. The results were $V_b = 125.2 \pm 5.3$ MeV, $R_b = 12.2 \pm 0.4$ fm (reduced $\chi^2 = 0.49$) for the $1/E$ plot and $V_b = 124.3 \pm 5.9$ MeV, $R_b = 11.9 \pm 0.7$ MeV from the coupled channels fit. The weighted averages of these quantities are $V_b = 124.8 \pm 0.3$ MeV, R_b

$= 12.1 \pm 0.1$ MeV. Thus one observes a lowering of the interaction barrier height and an increase in the interaction radius with the *n*-rich projectile of 5.9 ± 0.4 MeV and 1.8 ± 0.1 fm, respectively, in going from the ^{32}S projectile to the ^{38}S projectile.

How does this change compare with various semiempirical predictions of the isospin variation of these quantities?
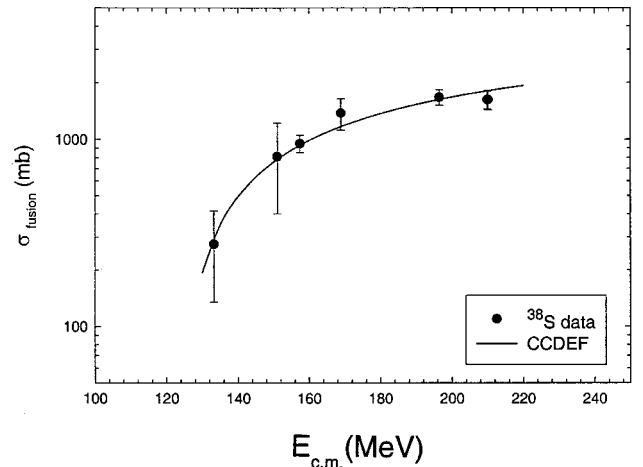

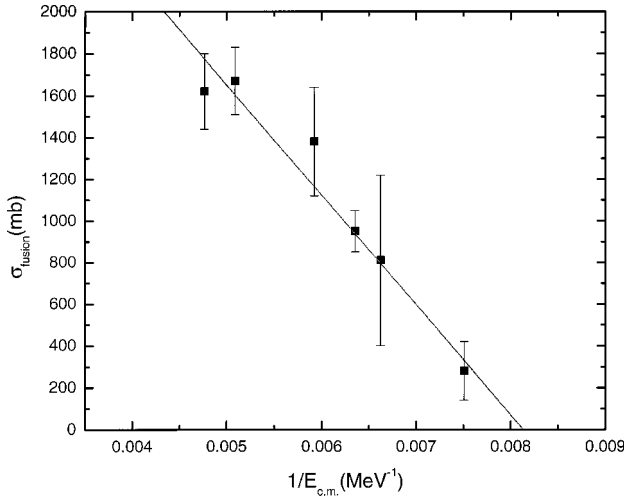FIG. 10. Measured capture fission excitation function for the ^{38}S$+^{181}$Ta reaction, showing a coupled channels fit to the data.

FIG. 11. $1/E$ plot for the ^{38}S$+^{181}$Ta capture fission excitation function.

The comparisons are summarized in Table II. The best agreement with the shift of the barrier height is with the predictions of Bass and Puri *et al.* [46]. In the case of the Bass model, the underestimate of the barrier shift has been noted before in the context of heavy element production reactions [7], where there is a trend of seeing maxima in cold fusion excitation functions shift more with increasing projectile isospin than one would anticipate based upon the Bass model. The large shift in the interaction radius would suggest that the simple one-dimensional potentials used in the models are not adequate to account for the effect of the increased deformation of the ^{38}S projectile ($\beta_2=0.246$) [39] relative to ^{32}S. This effect had to be included in the coupled channels calculation (along with the deformation of the target nucleus) to properly fit the data.

It is interesting to test whether there is any evidence in this data for anything other than a simple shift in the height of the fusion barrier as the projectile shifted from stable ^{32}S to neutron-rich ^{38}S. In Fig. 12, we show a reduced excitation function for the two systems. When the differences in barrier height and interaction radius are factored out, the data from the two systems are in agreement. Within experimental uncertainties, there is no evidence for any enhancement due to coupling to additional modes in the energy region measured.

What are the implications of this work for the synthesis of new heavy nuclei using *n*-rich projectiles? We have observed

TABLE II. Comparison of measured and predicted shifts in barrier parameters.

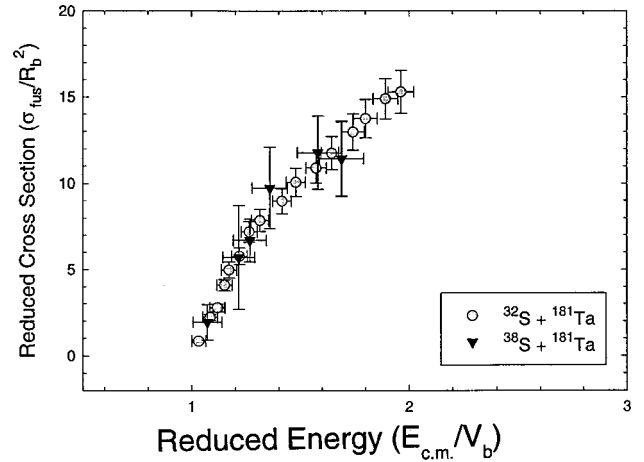|	ΔV_b(MeV)	ΔR_b(fm)
Experimental	5.9 ± 0.4	1.8 ± 0.1
Bass [42]	4.0	0
Vaz *et al.* [43]	3.8	0.3
Royer *et al.* [44]	3.1	0.4
Puri and Gupta [45]	3.3	7.6
Puri *et al.* [46]	8.0	0.9

FIG. 12. Reduced excitation functions for the $^{32,38}+$Ta reaction.

a shift of the barrier height of 5.9 MeV in going from ^{32}S to ^{38}S. In addition, the Q values of the reactions are -80.6 MeV and -86.9 MeV for the ^{32}S and ^{38}S induced reactions, respectively. This means that the excitation energy of the completely fused system is lowered by 12.2 MeV for the *n*-rich projectile compared to the stable projectile for the same fusion probability. This corresponds to evaporating one fewer neutron, with an increase in the *x-n* cross section of a factor of Γ_n/Γ_f, which can be a factor of 10–1000 [40]. An example of what this effect might mean for the synthesis of new heavy nuclei with radioactive beam facilities is shown in Fig. 13. We plot the calculated [41] cross section for the ^{252}Cf(^{X}Ne,4n) reaction as a function of the mass number of the projectile X. In this calculation, we assume a constant fusion cross section, but adjust the excitation energy by using the calculated values of Q for the reaction and assume fusion takes place at the Bass barrier. While one must ultimately consider the intensities of the very *n*-rich beams, significant increases in the production rates of very *n*-rich nuclei are predicted. These reactions, leading to new very long-lived heavy nuclei, could be of importance in the
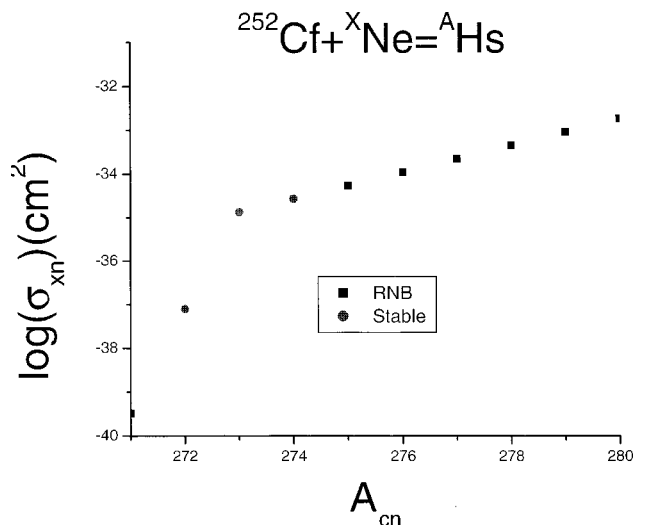

FIG. 13. Predicted cross sections for the ^{252}Cf(^{X}Ne,4n) reaction.

study of the atomic physics and chemistry of the heaviest elements.

IV. SUMMARY AND CONCLUSIONS

In conclusion, we believe we have shown that (1) it is possible to study the fusion of neutron-rich heavy nuclei using existing radioactive beam facilities, (2) the fusion barrier heights for neutron-rich nuclei are substantially lower than for nuclei near the valley of β-stability, and (3) the lowering of the fusion barrier height is large enough to significantly affect the synthesis of heavy nuclei.

[1] Nuclear Science: A Long Range Plan, 1996.

[2] W. Loveland, *Proceedings of the 3rd International Conference on Radioactive Nuclear Beams*, edited by D.J. Morrissey (Editions Frontieres, Gif-sur-Yvette, 1993), pp. 526–536.

[3] N. Takigawa, H. Sagawa, and T. Shinozuka, Nucl. Phys. **A538**, 221c (1992).

[4] N. Takigawa and H. Sagawa, Phys. Lett. B **265**, 23 (1991).

[5] M.S. Hussein, Nucl. Phys. **A531**, 192 (1991); Phys. Rev. C **44**, 446 (1991).

[6] C.H. Dasso and R. Donangelo, Phys. Lett. B **276**, 1 (1992); C.E. Aguilar *et al.*, Phys. Rev. C **46**, R45 (1992).

[7] G. Munzenberg, Philos. Trans. R. Soc. London, Ser. A **356**, 2083 (1998).

[8] M. Beckerman *et al.*, Phys. Rev. Lett. **45**, 1472 (1980).

[9] W. Reisdorf *et al.*, Phys. Rev. Lett. **49**, 1811 (1982).

[10] R. Broglia, C.H. Dasso, S. Landowne, and G. Pollarollo, Phys. Lett. **133B**, 34 (1983).

[11] H. Ernst, W. Henning, C.N. Davids, W.S. Freeman, T.J. Humanic, F.W. Prosser, and R.A. Racca, Phys. Rev. C **29**, 464 (1984).

[12] K.T. Lesko, W. Henning, K.E. Rehm, G. Rosner, J.P. Schiffer, G.S.F. Stephens, B. Zeidman, and W.S. Freeman, Phys. Rev. C **34**, 2155 (1986).

[13] K.E. Rehm, H. Esbensen, J. Gehring, B. Glagola, D. Henderson, W. Kutschera, M. Paul, F. Soramel, and A.H. Wuosmaa, Phys. Lett. B **317**, 31 (1993).

[14] A.M. Vinodkumar, K.M. Varier, N.V.S.V. Prasad, D.L. Sastry, A.K. Sinha, M. Madharan, P. Sugathan, D.O. Kataria, and J.J. Das, Phys. Rev. C **53**, 803 (1996).

[15] D. Ackermann *et al.*, Nucl. Phys. **A609**, 91 (1996).

[16] H. Timmers *et al.*, Phys. Lett. B **399**, 35 (1997).

[17] V.Yu. Denisov, GSI preprint 98-56, 1998; Yad. Fiz. **62**, 1431 (1999) [Phys. At. Nucl. **62**, 1349 (1999)].

[18] W. Reisdorf, J. Phys. G **20**, 1297 (1994).

[19] S.J. Skorka *et al.*, *Heavy Ion Fusion Reactions* (World, Singapore, 1984), p. 3.

[20] P.H. Stelson, H.J. Kim, M. Beckerman, D. Shapira, and R.L. Robinson, Phys. Rev. C **41**, 1584 (1990).

[21] A.M. Vinodkumar, A.K. Sinha, N.V.S.V. Prasad, K.M. Varien, and P. Sugathan, Phys. Rev. C **54**, 791 (1996).

[22] C. Signorini, Nucl. Phys. **A616**, 262c (1997).

[23] K.E. Zyromski *et al.*, Phys. Rev. C **55**, R562 (1997).

[24] The Isospin Laboratory, LALP-91-51.

[25] A. Gavron, Phys. Rev. C **21**, 230 (1980).

[26] D. Swan, J. Yurkon, and D.J. Morrissey, Nucl. Instrum. Methods Phys. Res. A **348**, 314 (1994).

[27] O. Batenkov *et al.*, Nucl. Instrum. Methods Phys. Res. A **394**, 235 (1997).

[28] V.E. Viola, Jr., T.D. Thomas, and G.T. Seaborg, Phys. Rev. **129**, 2710 (1963).

[29] Th. Rubehn, K.X. Jing, L.G. Moretto, L. Phair, K. Tso, and G.J. Wozniak, LBNL-38865.

[30] S. Schlomo and J.B. Natowitz, Phys. Rev. C **44**, 2878 (1991).

[31] B.B. Back, D.J. Blumenthal, C.N. Davids, D.J. Henderson, R. Herman, D.J. Hofman, C.J. Jiang, H.T. Penttila, and A.H. Wuosmaa, Phys. Rev. C **60**, 044602 (1999).

[32] J. Fernandez-Niello, C.H. Dasso, and S. Landowne, Comput. Phys. Commun. **54**, 409 (1989); C.H. Dasso and S. Landowne, *ibid.* **46**, 187 (1987).

[33] P. Möller, J.R. Nix, W.D. Myers, and W.J. Swiatecki, At. Data Nucl. Data Tables **59**, 185 (1995).

[34] S. Raman, C. Malarkey, W. Milner, C. Nestor, Jr., and P. Stetson, At. Data Nucl. Data Tables **36**, 1 (1987).

[35] R.H. Spear, At. Data Nucl. Data Tables **42**, 55 (1989).

[36] B.B. Back, Phys. Rev. C **31**, 2104 (1985).

[37] J.G. Keller *et al.*, Phys. Rev. C **36**, 1364 (1987).

[38] J.R. Huizenga, A.N. Behkami, and L.G. Moretto, Phys. Rev. **177**, 1826 (1969).

[39] H. Scheit *et al.*, Phys. Rev. Lett. **77**, 3967 (1996).

[40] T. Sikkeland, A. Ghiorso, and M. Nurmia, Phys. Rev. **172**, 1232 (1968).

[41] M. Cloughesy and W. Loveland, Phys. Rev. C (to be submitted).

[42] R. Bass, *Nuclear Reactions with Heavy Ions* (Springer, New York, 1980), pp. 283–351.

[43] L.C. Vax, J.M. Alexander, and G.R. Satchler, Phys. Rep. **69**, 373 (1981).

[44] G. Royer, C. Normand, and E. Druet, Nucl. Phys. **A634**, 267 (1998).

[45] R.K. Puri and R.K. Gupta, Phys. Rev. C **45**, 1837 (1992).

[46] R.K. Puri, M.K. Sharma, and R.K. Gupta, Eur. Phys. J. A **3**, 277 (1998).